Process Considerations for the Production of Hydrogen via Steam Reforming of Oxygenated Gases from Biomass Pyrolysis and Other Conversion Processes

Abhijit Dutta

In 2021, average CO_2 emissions was 9.7 g CO_2/g H_2 produced, primarily based on steam methane reforming (SMR) technology that currently dominates hydrogen production. The substitution of natural gas (NG) and other fossil feedstocks in SMRs with renewable gases may be considered as an option for reducing greenhouse gas emissions. This analysis explores process impacts and constraints associated with the potential introduction of biogenic gases into SMRs. The results indicate that replacing NG in the fuel train of the SMR, followed by partial replacement of NG in the feed train may be a feasible approach. For the CO- and CO_2-rich gas compositions assumed in this analysis the results indicate that feed train may accommodate up to 25 mole % of biogenic gases using allowances in existing designs and/or with small modifications, while maintaining similar hydrogen output. NG substitution in higher proportions require more major changes because of increased flow rates and heat exchange requirements in the system. Biogenic gases with lower CO_2 and higher calorific values are advantageous for NG substitution, and dry reforming using the CO_2 present in the feed gas can reduce steam consumption and increase process efficiency within limits where coking does not become a new constraint.

1. Introduction

Thermal conversion of biomass, such as via pyrolysis,[1] results in cracking and the production of gases. The proportions of various gaseous species are dictated by multiple factors, such as process configurations, catalysts used, and associated conditions. Except in processes where gas production is the goal (e.g., gasification processes), these produced gases are most often undesired byproducts. Upon biomass conversion, thermal or otherwise,

some of the oxygen inherent in the feedstock is usually included in produced gases (e.g., CO_2 in biogas; CO, CO_2, etc. in pyrolysis off-gas). Since the byproduct gases are biogenic, they have the sustainability benefits attributed to biomass feedstock. Thus, the judicious use of these renewably sourced gases to offset fossil derived energy, chemicals, and hydrogen can be a tool toward addressing the United Nation's Sustainable Development Goals,[2] by aiding sustainable transportation fuels and other industrial products.

The focus here is on the option to convert the produced gases to hydrogen via steam reforming. According to the International Energy Agency's tracking report for hydrogen,[3] ~82% of global hydrogen production in 2021 was from fossil fuels without subsequent carbon capture; the bulk of the remaining 18% of hydrogen produced was a byproduct from processes in the petrochemical industry, hence also primarily fossil derived. In 2021 global hydrogen production had a significant average CO_2 emissions footprint of 9.7 g CO_2/g H_2 produced.[4] In the US 99% of the hydrogen produced was from fossil sources, with steam methane reformers (SMR), accounting for 95% of the total production according to a July 2020 report.[5] Natural gas (NG) processing in SMRs has been the dominant technology for hydrogen production because of the availability of NG and the very favorable stoichiometry of its primary constituent (methane/CH_4) for H_2 production ($CH_4 + H_2O \leftrightarrow CO + 3 H_2$). CH_4 has the highest H:C ratio; additional H_2 is provided by steam, which also provides the oxygen needed to convert the C to CO. Since the current hydrogen production infrastructure is dominated by SMRs, the substitution of NG and other fossil feedstocks with renewable gases can be considered as an option. Compositions of renewable gases from the biomass processes usually differ significantly from hydrocarbon feedstocks such as NG. Previous analyses of pyrolysis processes have indicated that these gases may potentially be converted via steam reforming to produce sustainable hydrogen.[6,7] Other efforts are trying to produce hydrogen from these gases outside of traditional SMR configurations.[8] While the use of the hydrogen is not a focus of this article, the reader may note that the produced hydrogen

A. Dutta
Catalytic Carbon Transformation & Scale-Up Center
National Renewable Energy Laboratory
15013 Denver West Parkway
Golden CO 80401, USA
E-mail: abhijit.dutta@nrel.gov

available from biomass conversion facilities may be consumed locally or wherever a hydrogen transportation infrastructure will permit, including towards satisfying hydrogen demand for colocated hydroprocessing of biogenic intermediates to produce infrastructure compatible liquid transportation fuels,[7] such as sustainable aviation fuels (SAF).[9] Previously modeled estimates have shown significant greenhouse gas (GHG) benefits if fossil feedstocks can be substituted with renewable off-gases for hydrogen production, with one modeled example configuration showing GHG emissions for liquid biofuels production can be reduced by ~80% if pyrolysis off-gases are used instead of NG to produce hydrogen for hydroprocessing (Figure 4 in reference,[10]). Another recent analysis quantified the cost and sustainability impacts of using pyrolysis off-gases for different utility products, including hydrogen, electricity, and raw utilities such as steam and fuel gas; hydrogen production was shown to be an attractive option for pyrolysis off-gas use, based on the assumptions in that study.[11]

While SMRs using fossil feedstocks are well understood, there is current interest and modeling work on the reforming of sustainable feedstocks for hydrogen production, alternate processing configurations using options such as membrane reactors and chemical looping, and SMRs integrated with carbon capture, utilization, and storage (CCUS). A scan of the literature (not intended to be comprehensive) showed process modeling examples such as the use of biogas only as the SMR feed,[12,13] and combined use of NG and biogas with two separate reactors proposed for dry reforming of biogas and SMR of NG.[14] Other examples with process modeling and related analysis included the comparison of standard SMRs with alternate membrane SMRs,[15] SMRs with electricity production and CCUS.[16,17] Since pinch analysis is included in this study, the interested reader can also find studies such as one focused on the thermal efficiency of SMR processes that included pinch analysis as the centerpiece of the modeling.[18]

Given the multitude of studies on SMRs and related variations, it is important to point out the contributions of this study beyond previously published work reviewed by the author (acknowledging that some modeling studies may have been missed). This work was inspired by the author's previous work on biomass pyrolysis processes,[7] and the significant evolution of renewable off-gases in those processes. It is known that renewable hydrogen production from the off-gases can be beneficial and has synergy with the demand for hydrogen during the hydroprocessing of pyrolysis-derived oils to finished infrastructure compatible hydrocarbon fuels.[10] As with other renewable energy technologies, the reuse of existing infrastructure for renewable hydrogen production can have significant benefits towards reducing capital costs. For hydrogen, most of the current capital investment is in SMR systems and there may be an opportunity for SMR reuse with renewable gases/compatible feedstocks, including pyrolysis off-gases, and it is important to understand associated limitations. The simulation cases required to create the figures and results presented later in this article were developed to answer questions related to process constraints that will arise as feed gas quality, flow rates, heat integration, as well as any changes in temperature and pressure stretch the limits of an existing SMR system. Modeling details along with stream conditions are provided in the Supporting Information (SI) to enable others to quickly set up similar initial models, including for studies that may introduce other compatible alternate renewable carbon feeds.

2. Background and Methods

The analysis presented here should be viewed as an assessment tool for drawing objective conclusions; it is not intended to either encourage or discourage the adoption of any specific approach. The results highlight design considerations that may be important for partial or complete replacement of fossil hydrocarbon feedstocks in SMR-like configurations.

The base biogenic gas composition is derived from a modeled fast pyrolysis (FP) reactor yield as presented in PFD-61712-A201 of the appendix of a previous NREL report,[7]; the gases are separated after the FP products go through a condensation system to knock out liquid products. This model composition should not be viewed as generally representative of all pyrolysis processes. In fact, compositions of biogenic gases can vary significantly depending on the biomass type and process,[6,19] and even within the broad umbrella of pyrolysis process variants. While the base case model here has a CO_2:CO molar ratio of 0.87 in the PY gas, a sampling of some other work illustrates variations in CO_2:CO molar ratios: 0.42–0.62,[20] 0.34–0.44,[21] 0.60-1.52,[6] and 0.30-0.41.[22] Thus, off-gases from the family of pyrolysis processes can often have a lower CO_2:CO ratio compared to our base model value of 0.87. The methods discussed here can be adapted to study the process impacts of all such variations. To cover this key variation, a section of the results is dedicated to SMR process sensitivities related to CO_2:CO molar ratios. Deoxygenation is a key goal for pyrolysis processes targeting liquid transportation fuels as the primary product; in that context it should be noted that deoxygenation of biomass via CO_2 is preferable over the production of CO because two moles of oxygen are taken up with the loss of one mole of C in the case of CO_2, versus CO being half as efficient for deoxygenation. On the other hand, a higher proportion of CO (i.e., a lower CO_2:CO ratio) in the off-gas results in a higher calorific value of the gas and allows more hydrogen production via water gas shift, and is more efficient for hydrogen production.

For brevity, the remainder of this article refers to natural gas as NG, and pyrolysis off-gases as PY gas or PY. Note that although the abbreviation PY (pyrolysis) is used here, it may be reflective of other biogenic gas sources, since the sensitivity cases explore a range of gas compositions. Base case PY gas and NG compositions are shown in **Table 1**. NG compositions were kept constant throughout the analysis to help illustrate the other variations in this study without introducing additional variations related to NG composition.

For the CO_2:CO ratio sensitivity studies, the total molar proportion of (CO_2 + CO) in the PY gas was kept constant (as in Table 1), and the molar ratio of CO_2:CO was adjusted within that total proportion. Steam to carbon molar ratios (S:C), were calculated based on total carbon and total steam, without discounting carbon that is already fully oxidized and present as CO_2.

2.1. Steam Reforming of Biogenic Gases

Steam reforming of biogenic gases and heavier molecules (known as tars) after gasification has been an area of research

**ADVANCED
SCIENCE NEWS**

www.advancedsciencenews.com

**ADVANCED
SUSTAINABLE
SYSTEMS**

www.advsustainsys.com

Table 1. Compositions of PY gas and NG used in the model. The PY gas composition shown in this table should not be interpreted as a general representation of biomass pyrolysis derived gases because gas compositions vary significantly with processes and catalysts used.

Compound	Formula	PY gas [mole %]	NG [mole %]
Nitrogen	N_2		1.000%
Water (moisture)	H_2O	4.183%	
Carbon-monoxide	CO	44.577%	
Carbon-dioxide	CO_2	38.935%	0.300%
Methane	CH_4	6.688%	94.000%
Glyoxal	CH_2O_2	1.134%	
Ethylene	C_2H_4	1.900%	
Glycolaldehyde	$C_2H_4O_2$	0.084%	
Acetic acid	$C_2H_4O_2$	1.192%	
Ethane	C_2H_6		3.300%
Propylene	C_3H_6	0.073%	
Acetol	$C_3H_6O_2$	0.044%	
Propionic acid	$C_3H_6O_2$	0.041%	
Propane	C_3H_8		1.000%
1-butene	C_4H_8	0.064%	
n-butane	C_4H_{10}		0.400%
Furfural	$C_5H_4O_2$	0.060%	
Furfuryl-alcohol	$C_5H_6O_2$	0.031%	
Phenol	C_6H_6O	0.003%	
2-methyl-2-cyclopenten-1-one	C_6H_8O	0.091%	
2-hydroxymethyl-cyclopent-2-enone	$C_6H_8O_2$	0.003%	
Cyclohexanone	$C_6H_{10}O$	0.034%	
1-hexanal	$C_6H_{12}O$	0.256%	
2,5-dimethoxytetrahydrofuran	$C_6H_{12}O_3$	0.586%	
4-vinylphenol	C_8H_8O	0.009%	
2,4,6-trimethylpyridine	$C_8H_{11}N$	0.013%	

and has been demonstrated in the past.[23,24] In many respects pyrolysis off-gases are more amenable for gas processing because heavier molecules are scrubbed to recover liquid products before the gases are made available for other uses such as reforming.[7] Gasification processes operate at higher temperatures (typically >800 °C) and conceptual designs often include steam reforming before gas quench and condensation to avoid a significant temperature swing between the gasifier and the reformer (both operating at high temperatures),[25,26] although the reforming step may be skipped for very high temperature gasification at ≈1300 °C because of favorable equilibrium for the conversion of hydrocarbons and tars to CO and H_2.[27] On the other hand, lower severity thermal breakdown during pyrolysis (typically ≈500 °C) leaves small proportions of light molecules with CHO, in addition to often-dominant proportions of CO, CO_2, along with light hydrocarbon gases in the C1-C4 range; the C2-C4 hydrocarbons typically have high proportions of olefins. The presence of high proportions of CO, CO_2, and the smaller proportions of CHO molecules in the feed is not usual for SMR systems, hence some adaptations for handling them may be necessary. Besides the necessary process adaptations indicated via this analysis, there may be other considerations including the compatibility of process equipment and materials of construction for handling these alternate gas compositions.

Pre-reformers (before the main reformer) are included to allow feed flexibility in SMRs by converting most of the other molecular species to CH_4, CO, CO_2, H_2, and H_2O. Typically, pre-reforming reactions are targeted to approach equilibrium compositions at operating temperatures of 380–550 °C. The lower operating temperature, compared to the main reformer operations at higher temperatures (700–950 °C at the outlet), reduces coking propensity of feed constituents such as olefins.[28] The conversion of other species to the five primary species (CH_4, CO, CO_2, H_2, H_2O) helps achieve similarity with respect to the constituent gases usually handled in the main reformer at higher temperatures, although the proportions of the five constituents can vary significantly with feed gas compositions (especially with the introduction of biogenic gases). While a pre-reformer is typically designed for hydrocarbon feedstock flexibility, it can also potentially convert CHO molecules (oxygenates) from pyrolysis to the same five species before the main reformer, thus shielding the main reformer from having to handle any major new species.

It is important to note that biogas reforming (often with high CO_2 contents) is an important research area,[19] and learnings from that field may be applicable to other biogenic gases, especially for the design of catalysts that take advantage of CO_2 to help reduce steam requirement for pre-reforming and reforming. However, gasification- and pyrolysis-based systems are expected to be larger point sources of renewable gases and may have better scale-synergy with SMR systems compared to biogas; biogas is generally more distributed, although that may be overcome by adequate piping.

Key reforming, as well as water gas shift (WGS), reactions involving CH_4, CO, CO_2, H_2, and H_2O, and their heat effects have been discussed in many previous publications, including open-source references,[19] and not repeated here. With the introduction of other species and their conversion in the pre-reformer, additional heat effects are introduced. Those heat effects can be calculated through the heats of formation of individual species,[29] or using estimation methods when the data is not available.[30] Commercial process simulation software programs provide the ability to readily calculate these effects using built-in databases and estimation techniques. Studies on steam reforming of CHO species have been presented in the literature,[31,32] and they indicate general conformity with pre-reformer operating temperature ranges.

2.2. SMR System Design

There can be many variations in steam reformer designs.[28] This study uses one specific design configuration suitable for illustrating feed gas composition impacts. Inherent is an assumption that near-equilibrium conversions usually achieved in pre-reformers and reformers will hold for the CHO species included in the modeled PY gases. Near-equilibrium conversions are desirable and often indicative of efficient operations. The flow diagram for the design used in this study is shown in **Figure 1**. This was adapted from similar configurations presented in the literature.[33] The flow diagram includes heat integration implemented in the process model. Since SMR systems are mature, well known, and
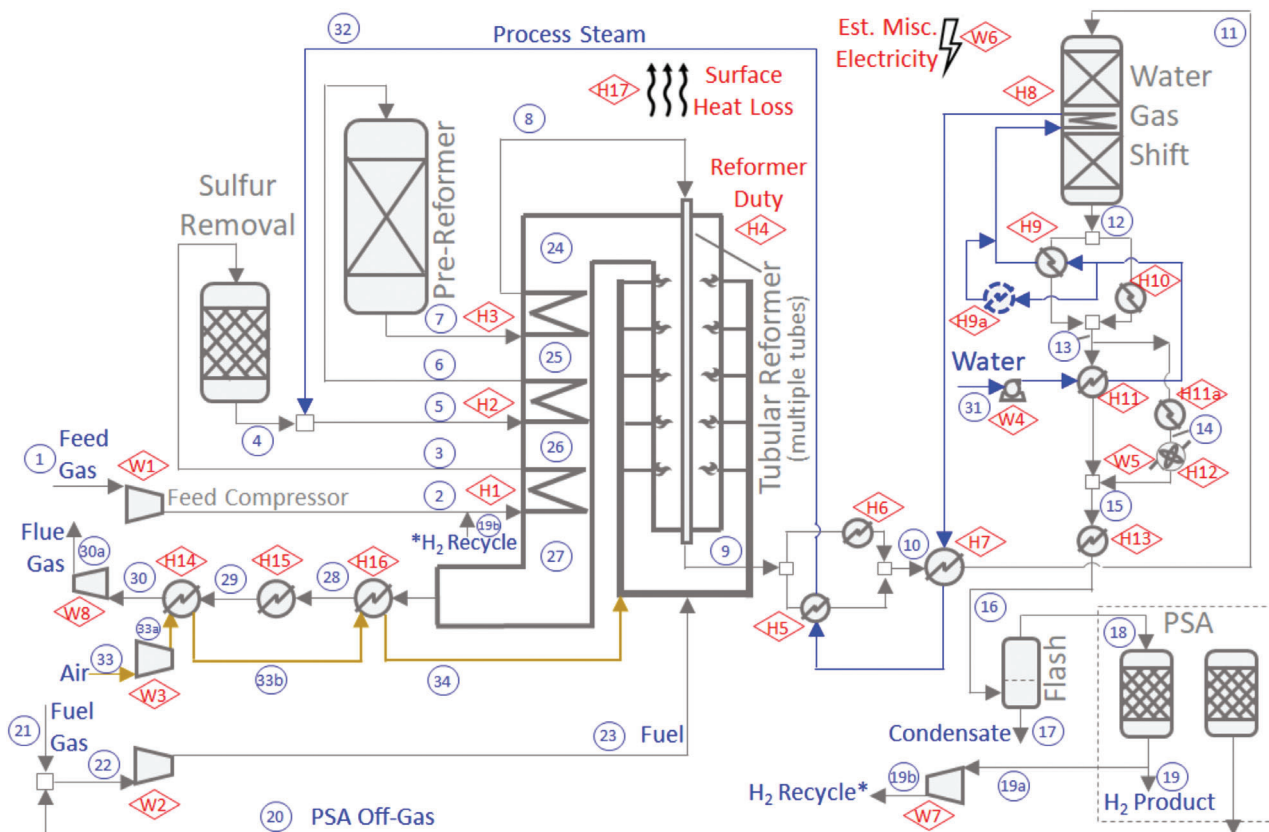
Figure 1. Process flow diagram. Circled tags are material stream numbers, tags within diamonds are for heat (H) and work (W). Additional descriptions of the tags are included in Table SI-1 (Supporting Information). Modeled values associated with the tags for systems with (i) NG and (ii) PY gas are included in Table SI-1 (Supporting Information).

documented for many decades,[28,33] only brief descriptions of key operations are included; most of the focus of the following writeup is on assumptions associated with the process model.

2.2.1. Process Modeling

The process model was built using Aspen Plus,[34]; built-in unit operations, including equilibrium reactors, heat exchangers, flash drums, separators, compressors, pumps, etc. were used in the model. Table SI-1A (Supporting Information) lists the unit operation blocks used in the model followed by detailed stream information corresponding to the block specifications. The Peng-Robinson Boston-Matthias (PR-BM) method was specified as the base property method. Steam table (STEAM-TA) was used for the streams with water specified as the only component (for steam generation). Pinch analysis for heat integration assessment was carried out in a spreadsheet, similar to previously published reports.[7,35]

The overall system is designed for ~25 bara (bar absolute) at the reformer, and the feed system assumes gas availability close to 2 bara for all gases, although NG may typically be available at higher pressures; compressor sizing and power need to be evaluated and adjusted based on gas supply pressures and compositions. Gas phase pressure increases were modeled using compressor models in Aspen Plus with default efficiencies of 72%.

The feed compressor was modeled with four stages and intercoolers at 82 °C, 93 °C, and 110 °C for all cases; intercooler temperatures were chosen to avoid having to change the model to account for condensation in cases with different feed gas compositions included in this analysis. The base model was developed to allow similar configurations and common assumptions for a variety of scenarios, rather than trying to examine optimizations for each specific feed gas composition. Temperatures and pressures at the various units are mentioned in the description below; the interested reader can see Table SI-1 (Supporting Information) to get additional information for the two modeled systems with NG and PY gas. Feed and fuel gas quantities were adjusted using design specifications in the model; the criterion for all the modeled cases is a fixed output of 5000 kg h^{-1} of pure hydrogen. This criterion allowed comparisons among various cases to help understand what process impacts need to be considered to maintain the same hydrogen production rate if the feed and fuel gas compositions are changed.

2.2.2. Economics and GHG Emissions

SMR cost estimates for fossil feed/fuel systems are available in the literature.[16,36] This article is focused on understanding process constraints that will arise from using alternate feed/fuel gases in SMRs. Once specific retrofits are identified to mitigate

**ADVANCED
SCIENCE NEWS**

www.advancedsciencenews.com

**ADVANCED
SUSTAINABLE
SYSTEMS**

www.advsustainsys.com

the identified constraints, preliminary cost estimates can be obtained via standard cost estimation tools for process equipment (e.g., the cost of resizing or replacing a compressor). Such estimation efforts can be detailed and subjective and should be considered only after narrowing down a few specific cases of interest; extensive cost estimation is not useful without the identification of plant objectives and corresponding modeled process feasibility. Thus, specific cost impacts are not elucidated in this paper, although select cases may be considered for cost studies as part of future work.

Direct CO_2 emissions, which are the bulk of GHG emissions from this process are shown in the results. These estimates are direct outputs from the process model (figures included in the results section below and further detailed stream information for the two bookend cases using NG and PY gases are shown in the Supporting Information). Additional energy use and export are documented and their GHG impacts may be calculated using emission factors included later in this article. However, since emissions associated with renewable gases can vary with the source and prior processing steps, any attempts to show GHG emissions for a broader scope will require significant additional information not directly relevant to SMRs and is not included in this paper; reported emissions and energy inputs/outputs are focused only around the SMR process.

2.2.3. Sulfur Removal

Sulfur removal includes a hydrogenator followed by zinc oxide beds for removing H_2S. Since woody biomass feedstocks have low sulfur and chlorine contents, their off-gases may not require significant modifications for these operations, other than to adjust for increased volumetric flow rates. Additional changes may be necessary for off-gases sourced from the conversion of other biomass feedstocks such as agricultural residues that contain more sulfur, chlorine, and other elements,[37]; the design and capacity of this unit should be scrutinized based on the quantities and types of sulfur species in the gas feed. For the current analysis this unit was modeled trivially using a separator block to remove H_2S after the hydrogenation of sulfur species. The parameter important for the process model was the specified temperature of 370 °C, that needs to be achieved through heat integration. 370 °C was chosen based on a recommended temperature range of 350–400 °C.[38] A slip stream from the produced hydrogen was recycled for the hydrogenator with a specification to maintain a 2% hydrogen level at its exit, a typical specification for systems using NG.[38]

2.2.4. Pre-Reformer

Adiabatic pre-reforming follows the sulfur removal step and is modeled as an equilibrium reactor. All the steam needed to meet the S:C ratio is introduced prior to the pre-reformer in this assessment; an S:C of 3 was maintained in all the cases, unless otherwise mentioned in the sensitivity cases that explore the impact of changes in S:C. The inlet temperature was set at 450°C in the model.[38] The introduction of oxygenated gases can significantly alter the temperature profile of this reactor, as shown

later, with endothermic operation for NG (modeled exit temperature 403 °C) switching over to an exothermic operation for PY gas (modeled exit temperature 583 °C), primarily because of significant exothermic water gas shift activity with the presence of CO in the feed. The reactor is also reported to be exothermic for naphtha feedstocks per an estimated exit temperature of 477 °C in the literature.[38] While the modeled exit temperature for PY gas (583 °C) is still close to the range of 350–550 °C mentioned in literature,[33] a more careful assessment is necessary for catalyst performance and maintenance to understand whether the exothermicity with PY gas warrants intermediate heat removal in the reactor.

2.2.5. Tubular Reformer

After the pre-reformer, the reformer inlet preheat temperature is set at 650 °C in the model; higher preheat temperatures may increase the risk of carbon deposition.[28] The modeled reformer outlet temperature is set at 880 °C, based on a range of 850–950 °C.[33] The model assumes equilibrium at the exit temperature of 880 °C. Note that the furnace provides the necessary heat (Figure 1). On the furnace side, 10% excess combustion air (oxygen) was specified in the model. The furnace was modeled at a negative gauge pressure (see Table SI-1F, Supporting Information for stream pressures) which is typical for safety reasons.[39] A balanced draft system with a forced draft fan for supplying combustion air and an induced draft exhaust fan for flue gas were included in the design.[40]

2.2.6. WGS

Since the WGS reaction ($CO + H_2O \leftrightarrow CO_2 + H_2$) is exothermic, an intercooler is included (Figure 1) for heat removal to maintain an exit temperature of 330 °C; medium temperature shift can have a range of 230–330 °C.[33]

2.2.7. Pressure Swing Adsorption (PSA)

The PSA system was modeled as a simple separator block with 85% recovery of hydrogen.[41] Changes in PSA inlet hydrogen concentration and increased gas volumes may warrant modifications to meet the 85% recovery specification; this aspect is not modeled in detail, but it is noted that the PSA module will require changes with any significant changes in gas compositions. In this analysis, pure hydrogen is reported in the product stream (steam 19 in Figure 1) and the plant design is fixed to produce 5000 kg h^{-1} of pure hydrogen.

Alternate designs for the purification of hydrogen, including acid gas removal and membrane systems are also implemented industrially, but not included in this analysis.

2.2.8. Heat Integration

Figure 1 shows the heat integration included in the model. Pinch analysis (results shown later for the NG and PY gas systems) was

**ADVANCED
SCIENCE NEWS**

www.advancedsciencenews.com

**ADVANCED
SUSTAINABLE
SYSTEMS**

www.advsustainsys.com

included in all the cases analyzed, to ensure that a feasible heat exchange network is possible based on the model specifications. A heat loss of 2% of the lower heating value (LHV) of the total fuel gas to the furnace was assumed in this analysis.

2.2.9. Electricity and Steam

Electricity consumption for compressors/fans (for feed, fuel, combustion air, and flue gas exhaust), the water pump, and air cooler were calculated in the process model; estimated miscellaneous extra requirements were set at 5% of the calculated total electricity consumption in the model.

Four qualities of steam were generated, based on extra heat duties available at different temperatures. A temperature difference of at least 40°C was maintained for all exchangers associated with steam generation. The four different steam pressures were 900, 350, 150, and 15 psig (62, 24, 10, and 1 barg respectively).

3. Results and Discussion

The process flow diagram (Figure 1) is annotated with tag names for material (circled numbers), heat (diamond tags starting with H), and work (diamond tags starting with W) streams. These tags are used to present key process details for two cases: (1) a base case with NG as feed (stream 1) and fuel (stream 21), and (2) a case with PY gas as both the feed and fuel. Modeled process values for these cases are detailed in Table SI-1 (Supporting Information). Note that the process model was set up to have a fixed hydrogen output of 5000 kg h^{-1}, with the general setup remaining the same, unless some alterations (mentioned later) were necessary in some cases to ensure there were no temperature crossovers during pinch analysis. Detailed mass and energy flows for the two cases are included in the Supporting Information, along with overall mass (Table SI-1B, Supporting Information) and energy balance summaries (Figures SI-1A,B, Supporting Information).

3.1. Model Validation for the NG Case

The model results for the NG case were compared with values for the base case reported in a 2017 IEAGHG report.[16] Note that the IEAGHG report was not used as a reference during model development and thus could be used for an independent validation. The IEAGHG report was prepared by Amec Foster Wheeler and based on the Foster Wheeler Terrace Wall reformer design. Not all process details were presented in the IEAGHG report, but there was sufficient information to allow a basic comparison. Some of the metrics from the comparison are presented in Table SI-1U (Supporting Information) and the notable differences (other than the choice of production capacity) are explained here. The molar ratio of hydrogen produced to input (fuel + feed) was 2.63 versus 2.69 in the model, validating the general production efficiency predicted by the model. A major difference was noticed in the ratio of NG feed to fuel, which was 6.06 in the IEAGHG report versus 11.10 in the model. The higher feed to fuel ratio was primarily because of the assumption of a PSA hydrogen recovery efficiency

of 85% in the model versus 90% in the IEAGHG report (note that IEAGHG report also states that typical PSA recoveries are in the 85–90% range). Upon changing the PSA recovery to 90% in the model (result shown in Table SI-1U, Supporting Information), as a sensitivity study (note that 85% recovery is used for all the other model results reported in this study), the feed to fuel ratio changed to 7.09, which is closer to the 6.06 value in the IEAGHG report. Note that PSA off-gases are used as fuel, thus reducing fresh fuel demand, consistent with lower fuel demand for the 85% recovery case versus the 90% case. Further, the IEAGHG report configuration coproduces electricity, and their heat integration was designed to produce high pressure steam compatible for use in a steam turbine. The model presented in this paper uses similar quality (temperature) heat to preheat air (instead of making steam) in order to increase thermal efficiency to help boost hydrogen production, which explains the higher feed to fuel ratio (7.09 in the model with a 90% Hydrogen recovery assumption) and also the slightly higher hydrogen produced for the same input of feed + fuel (ratio of 2.69 vs 2.63 mentioned above) compared to the IEAGHG report. Another major difference was in the reported electricity consumption, and this was attributed to the assumed feed supply pressure. As also mentioned elsewhere in this paper, a fuel supply pressure of ∼2 bara was assumed for all cases in the model, whereas NG supply headers are typically already at elevated pressures, and do not require additional compression. Eliminating the NG feed compressor and fuel compressor for the NG case removed the major sources of discrepancy in electricity requirements between the model and IEAGHG report. Note that the results reported in this paper are still based on a ∼2 bara feed/fuel supply pressure assumption; the granularity of information provided in all the plots and the tables in the Supporting Information will allow the reader to subtract contributions from NG compression in the relevant cases. Overall, the NG case in the model matched the reported metrics in the IEAGHG report, and there are logical explanations for the major differences noted above.

3.2. Pinch Analysis

There are significant differences between NG and the PY gas compositions for the base case in this analysis (Table 1). Notably, the estimated LHVs of NG and PY gas used in the base case were ∼48 500 and ∼7600 kJ kg^{-1} respectively. This translates into larger quantities (mass and volume flows) of gas required to satisfy both feed and fuel needs to maintain a 5000 kg h^{-1} hydrogen production capacity. Since process conditions (temperatures and pressures) are similar for the two modeled cases, the higher flow rates with PY gas results in higher overall thermal energy being carried through the process, needing larger heat exchange capacities. This is reflected by the total intra-process exchange duty shown by pinch analysis (**Figure 2**)

These two cases show the extremes of this comparative assessment, with all NG in both the feed and fuel trains in the first case completely replaced by PY gases in the second case. In reality, only partial replacement of NG may be considered in existing SMR systems, since the changes with full replacement of NG with PY gas are significantly beyond the 10–15% design allowances that may be available in any system or accomplished through some modifications within the same equipment
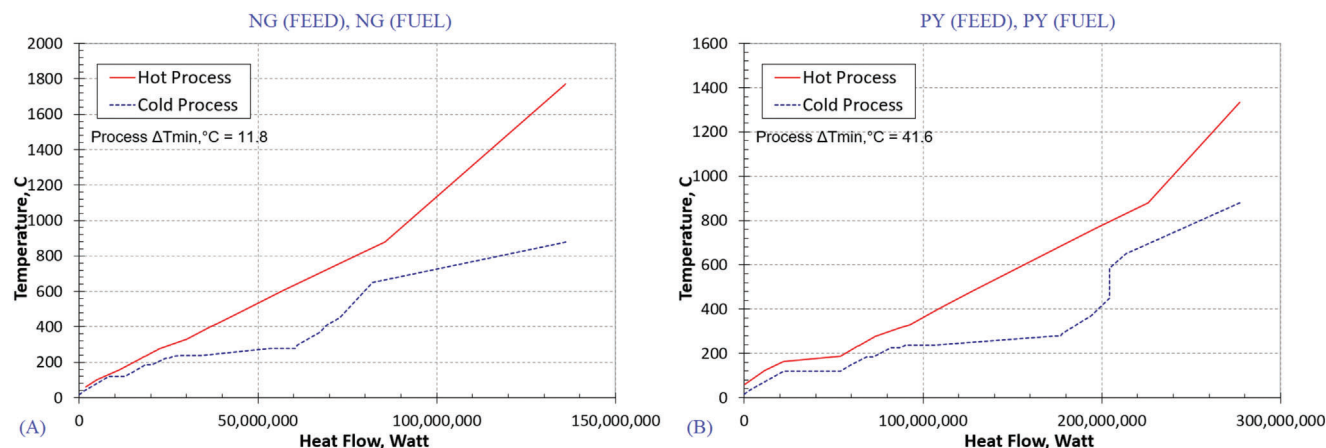
Figure 2. Pinch analysis for intra-process process heat exchange (air and water coolers not included) for A) NG as both feed and fuel, B) PY gas as both feed and fuel. The hottest furnace temperatures (right extremes of the hot process curve) reflect adiabatic temperatures possible in the reformer furnace; the highest temperatures will be tempered in an actual system because of simultaneous heat exchange with the endothermic reformer tubes. Air and water cooler duties reflect necessary losses for this modeled system design and are shown in Table SI-1 (Supporting Information) for the two cases. In addition, surface heat losses are modeled as 2% of the lower heating value of the furnace fuel gas. Similar pinch analysis was performed for all model runs to ensure that there were no temperature crossovers in any of the cases presented. Pinch points in the models were in the water preheat train for all the cases.

footprints. Flow rate increases beyond design allowances require adjustments to maintain reasonable pressure drops and catalyst reactivity which need to be addressed via larger piping and reactor volumes, and catalyst load increases; increased heat duties require larger heat exchange areas, and furnace fuel and air capacities; increased flow rates will also require larger compressors, air coolers, and other electrical equipment and result in higher electricity consumption. Complete redesign will thus be necessary for full transition from NG to PY gas while maintaining hydrogen production capacity; alternatively existing SMR systems may work with simpler modifications if hydrogen production capacity is reduced when using substantial proportions of PY gas.

The two extreme cases are presented as bookends of this impact assessment. The continuum of how various process parameters will be affected by a partial to complete transition from NG to PY gas is presented in the following sub-section. It should be noted that pinch analysis results are dictated by heat integration assumptions and the profiles shown in Figure 2 should be interpreted in the context of the process flow diagram in Figure 1. Many pinch analyses curves shown in the literature do not extend to process heat integration at lower temperatures such as water preheat included in this study, hence their global pinch points are at higher temperatures compared to the low-temperature pinch points shown in Figure 2.

3.3. Impact of Introducing Pyrolysis Off-Gases

NG may be substituted with PY gas on the (1) feed side only (**Figure 3**, Subset I), (2) both fuel and feed sides (Figure 3, Subset II), and (3) fuel side only (Figure 3, Subset III). The substitution may be partial in various proportions based on gas availability and production capacity. Since all carbon is converted to CO_2 in this system design, total CO_2 emitted is also an indicator of system design volume requirements.

Process impacts are captured through the summary plots in Figure 3. The impacts are dominated by changes on the feed side rather than fuel side, hence the similarities in overall patterns for Subset I and Subset II, which are discussed together below.

Plot A (in subsets I and II) shows the decline in fossil carbon and the increase in biogenic carbon emissions as the mole fraction of renewable PY gas is increased. As is expected fossil emissions go down to zero for a system operated completely with PY gas (Subset II). The increase in total emissions is due to (a) the larger flow and energy footprints as PY gas is increased (discussed above), (b) the presence of CO_2 in the PY gas which gets included with the final emissions. The emissions contribution from CO_2 already present in the PY gas (feed and fuel) is subtracted from the total in the "Net" emissions shown in Plot A.

Plot B (in subsets I and II) shows the quantities of steam produced at the four pressures; note that negative values are for steam production. The amount of the high pressure steam (900 psig) declines, and all the lower pressure steam (350, 150, 15 psig) increase as the proportion of PY gas is increased. The amount of lowest pressure steam (15 psig) increases the most and is shown on separate axes for Subsets I and II. Note that these changes are based on constraints of maintaining a feasible heat exchange network verified via pinch analysis and achieved within the model through appropriate specifications; the interested reader can follow further details of the specifications and impacts through Figure 1 and Table SI-1 (Supporting Information).

Plot C (in subsets I and II) shows the increase in electricity consumption as the system gets larger with the increase in the proportion of PY gas and associated increases in flow rates through compressors and other electricity-driven equipment.

Plot D (in subsets I and II) captures gas compositions at the pre-reformer outlet. As mentioned earlier, the pre-reformer converts the various molecular species in the feed gas into five primary constituents (CH_4, CO, CO_2, H_2, H_2O). This compositional

ADVANCED
SCIENCE NEWS

www.advancedsciencenews.com

ADVANCED
SUSTAINABLE
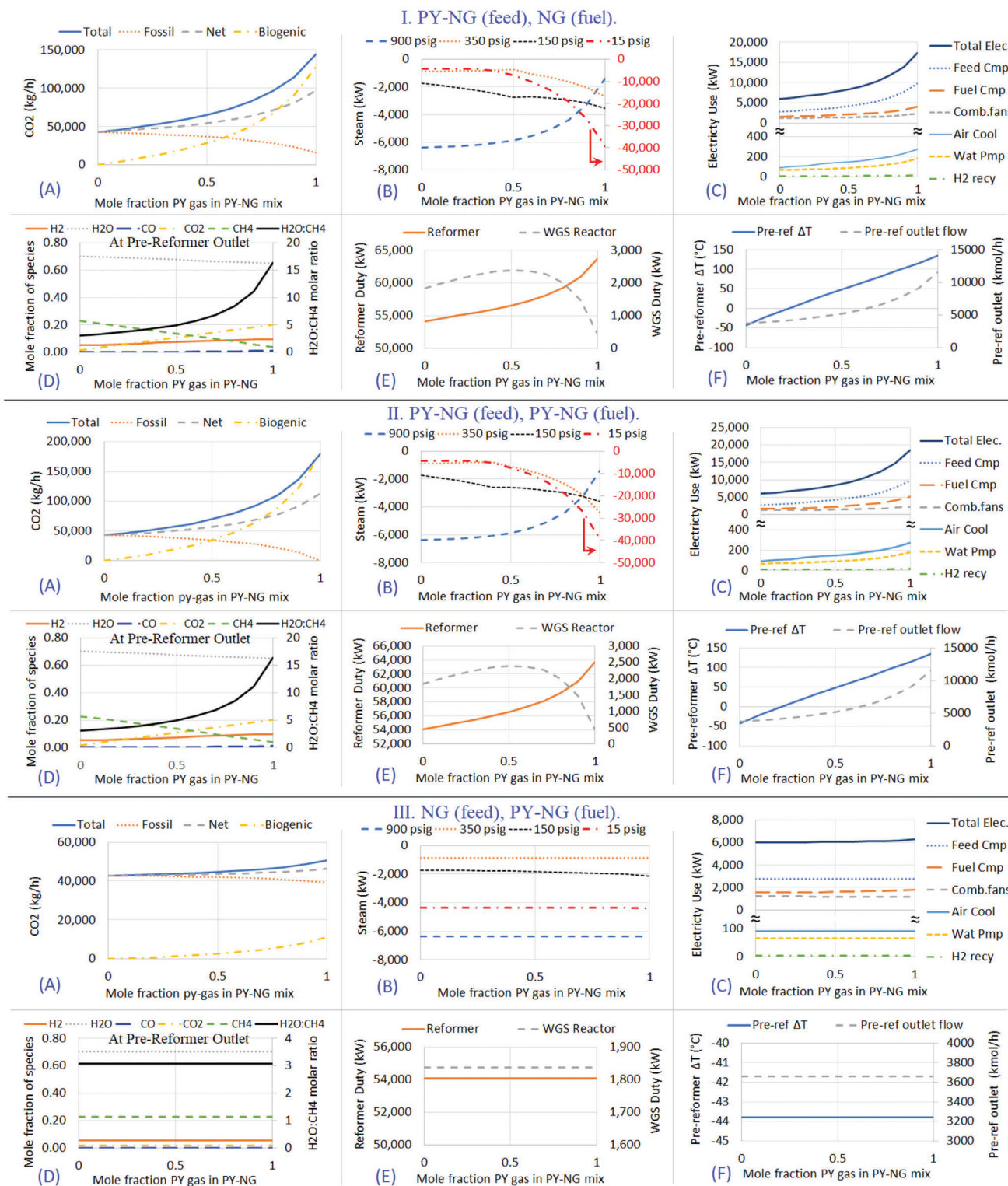**SYSTEMS**

www.advsustainsys.com

Figure 3. Impact of replacing NG with PY gas, with mole fractions of PY gas in the NG-PY gas mix varied from 0 to 1 in increments of 0.1. **Subset I**: PY gas replacement only on the feed side; **Subset II**: PY gas replacement on both feed and fuel sides; **Subset III**: PY gas replacement only on the fuel side. S:C of 3, and 10% excess air was maintained for fuel combustion in all cases. Any discontinuities in the plots are due to adjustments in temperatures in some of the models to avoid temperature crossovers or low ΔT_{min} detected during initial pinch analysis. Plot A: CO_2 emissions, Plot B: steam produced (negative values indicate production), Plot C: electricity consumption (additional 5% for miscellaneous usage included in total), Plot D: gas composition at the pre-reformer outlet and reformer inlet, Plot E: reformer and WGS reactor duties, Plot F: pre-reformer temperature change and outlet molar flow. Abbreviations: Cmp = compressor/blower, Elec = electricity, Comb = combustor, Pmp = pump, recy = recycle.

**ADVANCED
SCIENCE NEWS**

www.advancedsciencenews.com

**ADVANCED
SUSTAINABLE
SYSTEMS**

www.advsustainsys.com

plot captures how oxygen present in the PY gas species (Table 1) impacts the feed to the main reformer. $H_2O:CH_4$ molar ratios are on the secondary y-axis showing the significant change in this metric if the same S:C ratio of 3 is maintained (as mentioned earlier the S:C calculations were based on raw carbon and did not discount the carbon present as CO_2 in the feed); $H_2O:CH_4$ is an important parameter from a process standpoint because it can impact coking and have an impact on process efficiency. S:C sensitivity cases are thus discussed in a separate section below, where it indicates that there may be benefits of using a lower S:C ratio for PY gases.

Plot E (in subsets I and II) shows that the main reformer duty increases with the increase in PY gas proportion. Note that this duty also includes sensible heat required to heat the reformer feed from 650 °C at the inlet to 880 °C at the outlet; the required sensible heat plays a more dominant role as flow rates increase with the increase in the proportion of PY gases. The duty of the WGS reactor (exothermic) is shown on the secondary y-axis. The duty decreases as the conversion reduces in the WGS reactor; as the proportion of steam increases (Plot D) the reaction ($CO + H_2O \leftrightarrow CO_2 + H_2$) progresses further to the right even at the high temperature (880°C) in the reformer, before the WGS reactor, thus lowering the remaining activity in the WGS reactor.

Plot F (in subsets I and II) shows the temperature change in the adiabatic pre-reformer. As the proportion of PY gas increases, the reactor shifts from endothermic to exothermic. This increased temperature change may be beyond design considerations for the catalyst and may thus need to be controlled via an intercooler, moving away from a completely adiabatic design assumed in the base model; this was discussed in Section 2.2.4. The secondary axis on Plot F shows the molar flow rate. This reemphasizes the previous discussion about the increase in flow rates and volumes when PY gas (with the composition in Table 1) replaces NG as the feed.

Subset III in Figure 3 shows the impact of replacing NG with PY gas as the fuel to the reformer furnace. There is minimal overall impact, with relatively small changes as PY gas is used to replace NG as the fuel. Fossil emissions decrease, but to a smaller extent compared to the cases when feed is replaced as well, because fuel consumed is significantly less than the feed. Overall, plots A-F show very little potential disruptions with this approach. The excess air (oxygen) for combustion is still maintained at 10%. Oxygen present in the PY gas fuel is accounted in the combustion air calculations, lowering air input requirements (which has a positive impact on efficiency). Plot C shows that even though the fuel volume (indicated by the fuel compressor power) goes up, the air requirement remains nearly constant (indicated by fan power) with an increase in the proportion of PY gas.

From a high level it may be inferred upon examining Figure 3 that if sufficient PY gases are available, replacement of the entire fuel stream NG with PY gases and the inclusion of up to 25 mole % PY gas in the feed gas, will not result in significant disruptions in existing NG based systems, while still benefiting with respect to fossil emissions reduction associated with the use of PY gases. A sharp exponential increase in all process parameters is visible (Figure 3) after 50 mole % inclusion of PY gases (with the assumed PY gas composition). Caution should be used, and specific implementations need to be further scrutinized because this analysis focuses only on overall process

impacts. Equipment, catalyst, and material impacts from varying gas molecular species are not examined in detail, beyond the inclusion of their thermodynamic properties to understand process impacts. It should also be noted that these conclusions will change if there are significant deviations from the PY gas composition shown in Table 1; some potential compositional impacts are shown later in Section 3.5.

3.4. Impact of S:C Molar Ratio

Steam is necessary in an SMR system: (a) for providing oxygen needed to convert carbon to its oxides and prevent coking and (b) as a source of hydrogen. A stoichiometric reevaluation of the impact of the inclusion of oxygenated molecules in the feed indicates a reduced amount of steam may be necessary to prevent coking, because carbon oxides can form by utilizing oxygen in the feed molecules. However, unlike the utilization of oxygen during combustion, coking depends on many other factors including the temperature, proportion of hydrogen available, and molecular species present in the feed, thus experimental studies and caution are recommended before making changes. A carbon limit diagram showing potential changes in S:C in the presence of CO_2 was presented in the literature.[28] Adequate steam should be provided to reduce coking and optimize hydrogen production, with the consideration that excess steam reduces efficiency because of additional energy requirements. The impact of S:C on the process is shown in **Figure 4**.

Subset I (Plot A) shows that the lowest fossil CO_2 emissions (within the 1–3 S:C range explored) occurs at the lowest S:C of 1 with PY gas as feed (and NG as fuel), which is to be expected from an energy use standpoint. However, as mentioned earlier, coking can be a problem at low S:C ratios and experimental verification is necessary before lowering the S:C ratio for this PY gas composition. Plot D indicates that $H_2O:CH_4$ ratios are adequate at the reformer inlet, but the pre-reformer may be at risk of coking. Coking risks and catalyst choices may also be informed by experimental research on dry reforming ($CH_4 + CO_2 \leftrightarrow 2\ CO + 2\ H_2$), e.g., for biogas.[19] In this context it should be noted that use of CO_2 with reduced steam may be more beneficial for the production of syngas (since both CO and H_2 are desirable components of syngas); more steam may benefit maximization of hydrogen production via WGS to convert CO to H_2. Besides more energy use for steam production, higher $H_2O:CH_4$ ratios require downstream condensation of the excess steam and the removal of lower quality (lower temperature) heat. Even if the waste heat can be reused, excess heat exchanger capacity requires more capital investment. Catalyst sintering may be a potential problem with significant excess steam.

Subset II shows that the model results are aligned with conventional practice of industrial operations with S:C of ~3 for NG systems. While there may be marginal benefits of operating at a lower S:C of 2.5 (based on equilibrium conversion), there may be increased risk of coking at lower S:Cs.

3.5. Impact of PY Gas $CO_2:CO$ Mole Ratio

As discussed in Section 2.0, $CO_2:CO$ ratios can vary in biogenic gases and this section presents the impacts of the variations. Model results are presented in **Figure 5**.

2300241 (9 of 14)

**ADVANCED
SCIENCE NEWS**

www.advancedsciencenews.com

**ADVANCED
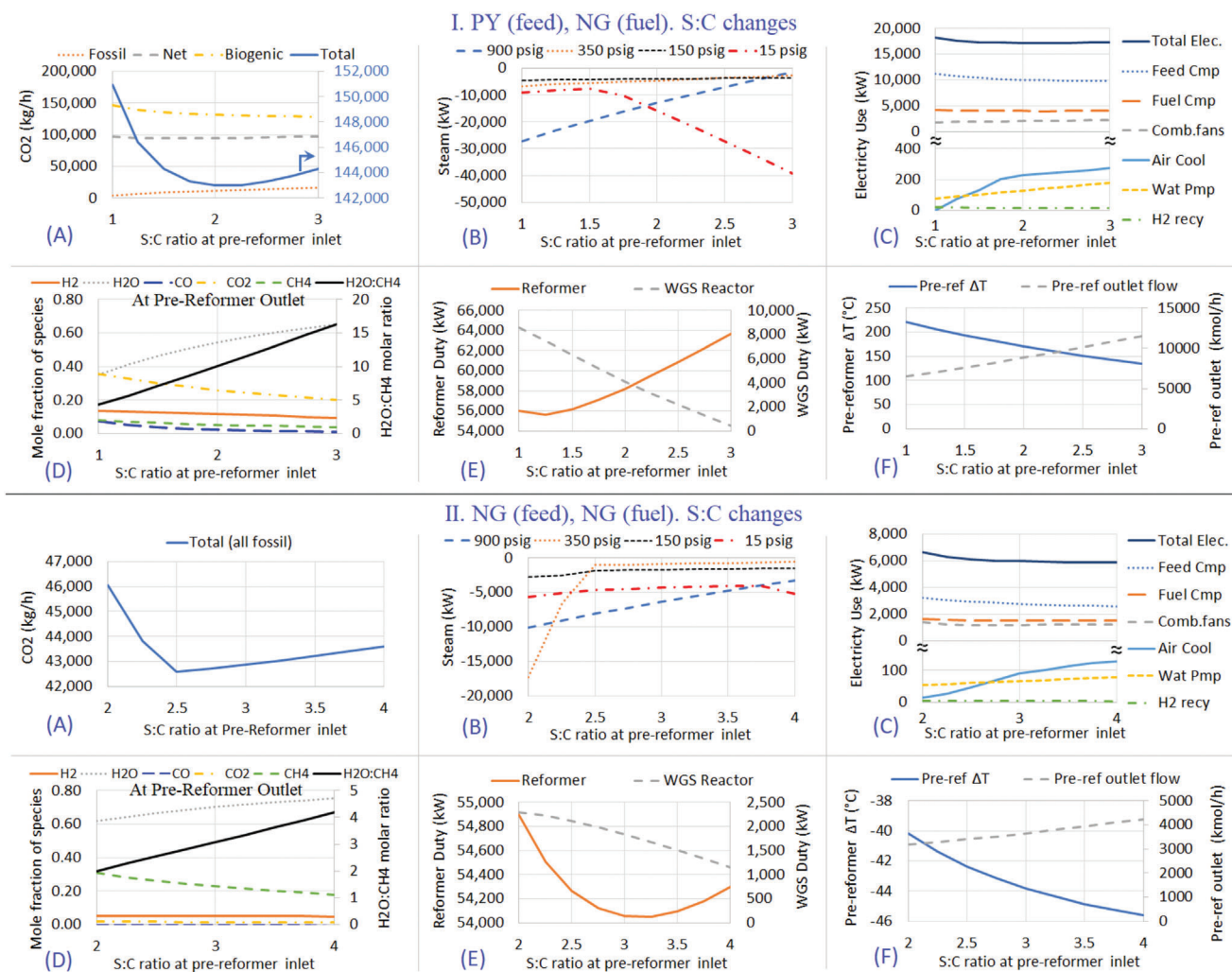SUSTAINABLE
SYSTEMS**

www.advsustainsys.com

Figure 4. Impact of S:C (steam to carbon ratio) on process variables. Subset I: PY gas as feed and NG as fuel, with S:C varied from 1 to 3 in increments of 0.25; Subset II: NG as feed and fuel, with S:C varied from 2 to 4 in increments of 0.25. 10% excess air was maintained for fuel combustion in all cases. Any discontinuities in the plots are due to adjustments in temperatures in some of the models to avoid temperature crossovers or low ΔT_{min} detected during initial pinch analysis. Plot A: CO2 emissions, Plot B: steam produced (negative values indicate production), Plot C: electricity consumption (additional 5% for miscellaneous usage included in total), Plot D: gas composition at the pre-reformer outlet and reformer inlet, Plot E: reformer and WGS reactor duties, Plot F: pre-reformer temperature change and outlet molar flow. Abbreviations: Cmp = compressor/blower, Elec = electricity, Comb = combustor, Pmp = pump, recy = recycle.

Note that the CO_2:CO mole ratio for the base case is 0.87 (Table 1). As mentioned earlier the total molar proportion of (CO_2 + CO) in the PY gas was kept constant at 83.5% (as in Table 1), and the CO_2:CO molar ratio was shifted within that total; ratios used in the model were 0.25, 0.5, 1, 2, and 4 with respective LHVs of 10473, 8954, 7272, 5789, and 4724 kJ kg^{-1}. As expected, the LHV of the gas decreases with an increase in CO_2:CO. As seen in the previous cases there are benefits of using feed gases with higher calorific value (i.e., lower CO_2 in the feed gas). All three subsets (I, II, III) in Figure 5 reflect this. Lowest total emissions (Plot A) are thus for the case with a CO_2:CO ratio of 0.25. The quantities of lower pressure steam (Plot B) also increase at higher CO_2:CO ratios in subsets I and II (note the significantly higher amount of 15 psig steam shown using the secondary y-axis). Unless the low pressure steam can be used efficiently for local consumption, higher amounts of low pressure steam translate to

lower efficiency of the overall process. Subset III reflects the use of PY gas on the fuel side only. As discussed earlier in Section 3.3, changes on the fuel side alone may be less disruptive because the oxygen present in the PY gas (as CO_2, CO, and molecules containing CHO) can be accounted and utilized to lower the combustion air (oxygen) requirement, thus helping mitigate some of the impacts of the lower LHV PY gas. Note that the discontinuities in Plot E for the WGS duty are because of adjustments to the WGS reactor inlet temperatures that were necessary to avoid temperature crossovers detected during pinch analysis for some of these cases.

The benefits of lower CO_2:CO ratios points to the potential benefit of removing CO_2 prior to introducing the gases to the reformer system, especially on the feed side. This can help keep the system flow rates and volumes closer to those in the NG system, and allow higher proportions of PY gas substitution within
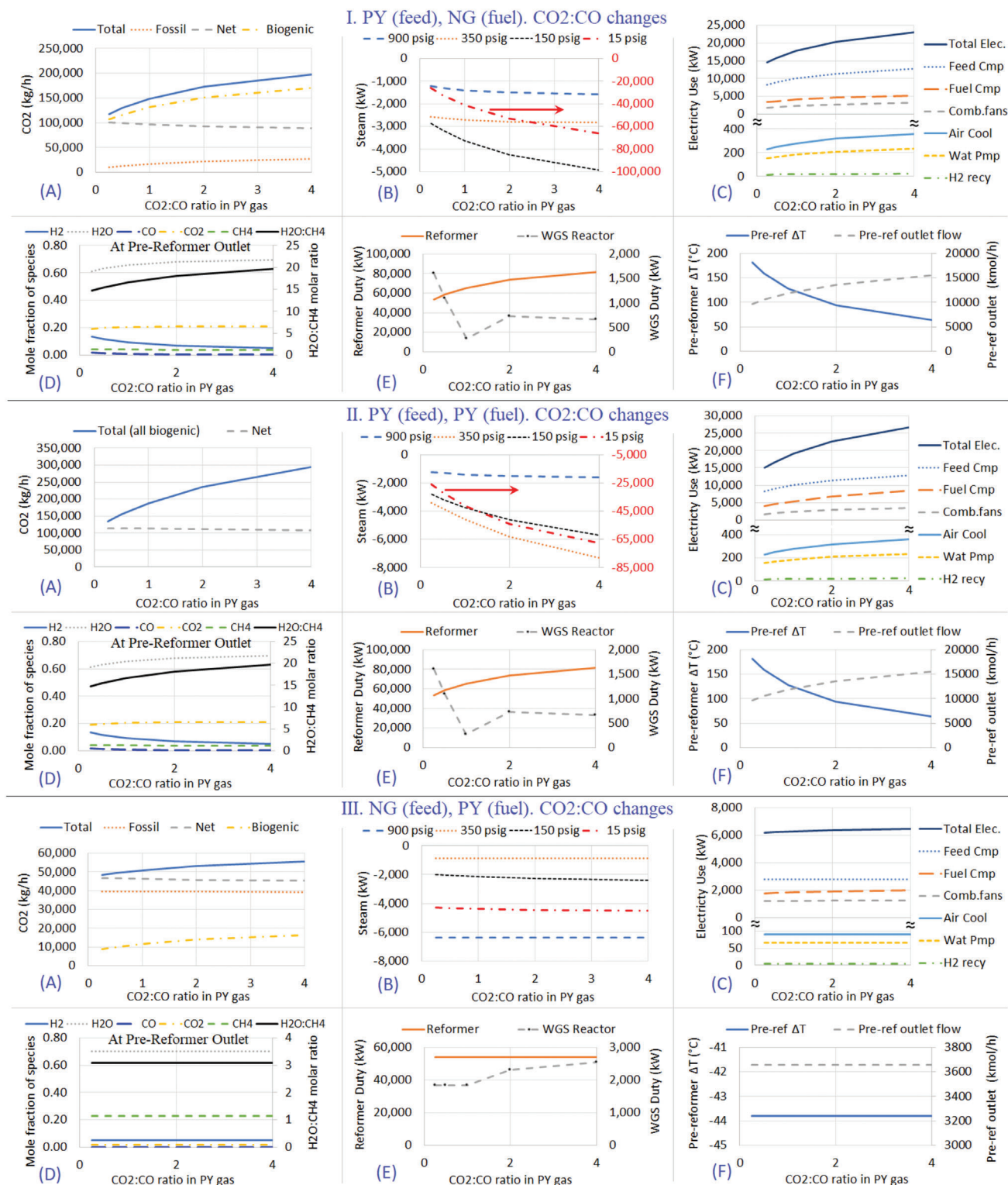
Figure 5. Impact of CO_2:CO molar ratios on process variables. Results are for CO_2:CO ratio values 0.25, 0.5, 1, 2, and 4. Subset I: PY gas as feed and NG as fuel; Subset II: PY gas as feed and fuel; Subset III: NG as feed and PY gas as fuel. Discontinuities in plots E are due to adjustments in WGS reactor inlet temperatures in some of the models to avoid temperature crossovers detected during initial pinch analysis. S:C of 3, and 10% excess air was maintained for fuel combustion in all cases. Plot A: CO_2 emissions, Plot B: steam produced (negative values indicate production), Plot C: electricity consumption (additional 5% included for miscellaneous usage included in total), Plot D: gas composition at the pre-reformer outlet and reformer inlet, Plot E: reformer and WGS reactor duties, Plot F: pre-reformer temperature change and outlet molar flow. Abbreviations: Cmp = compressor/blower, Elec = electricity, Comb = combustor, Pmp = pump, recy = recycle.

**ADVANCED
SCIENCE NEWS**

www.advancedsciencenews.com

**ADVANCED
SUSTAINABLE
SYSTEMS**

www.advsustainsys.com

the constraints of existing SMR system designs. However, there is an energy penalty for removing CO_2 and a broader analysis (that includes CO_2 removal cost and energy) is necessary before choosing such an option. Another potential concern with PY gases (that needs to be experimentally tested) is the possibility of degradation of solvents used for CO_2 removal due to the presence of molecular species that may be uncommon in typical CO_2 removal applications. Also, if a high proportion of CO is present in the gas, a lower cost option for hydrogen production that should be evaluated is the use a WGS reactor alone to maximize hydrogen and then purify the stream using a PSA or other means.

3.6. GHG Emissions

Direct CO_2 emissions, with contributions from fossil and biogenic sources are shown in Plot A in each of the figures. As discussed previously for each of the cases (a) fossil CO_2 emissions are reduced with the introduction of PY gas, (b) CO_2 emissions are reduced with the use of less steam because of reduced energy consumption associated with steam generation, (c) CO_2 emissions are reduced with a lower CO_2:CO ratio in the feed PY gas because the energy density of the gas goes up when there is less CO_2 present.

There are GHG emissions associated with sourcing feed gases. According to GREET 2022,[42] emissions associated with NG production are ~39 g CO_2e kWh^{-1}. PY gas emissions are expected to be biogenic, but the overall process may be impacted by design and operational choices such as the use of grid electricity and supplemental NG. Electricity consumption also has associated GHG emissions, ~0.45 kg CO_2e kWh^{-1} (for a U.S. mix) and steam produced, using a NG boiler, results in GHG emissions of ~0.3 kg CO_2e kWh^{-1}.[42] There are also emissions associated with other raw materials (such as catalysts) and ancillaries for the SMR process. All these emissions or credits (for steam production) need to be added to account for the overall GHG impact of hydrogen production. More low-quality (i.e., low-temperature) heat needs to be dissipated with an increase in the proportion of PY gas (Plots B in subsets I and II in Figure 3). Some of it can be recovered as low-pressure steam as shown in Figure 3. It may be difficult to find local consumers for large quantities of low-pressure steam or low-quality heat; colocation with biomass feedstock processing facilities may help in this regard because some of the low-quality heat may be used for the drying of biomass, such as wood used in fast pyrolysis. There can be significant additional GHG benefits if this low-quality heat can be used to replace NG for drying biomass. Steam credits can also help offset GHG impacts from increased electricity consumption associated with the use of PY gas (Plots C in subsets I and II in Figure 3).

3.7. Cost Impacts

Increased flow rates with the use of PY gas will require larger equipment. Depending on current operational status and constraints, there may be some flexibility in using design allowances to accommodate the substitution of a portion of NG with PY gas via relatively minor modifications. However, it may become infeasible to make accommodations within an existing NG SMR plant while maintaining the same hydrogen output. A complete redesign is necessary for a complete switch to PY gas since many of the process parameters increase significantly compared to the case using NG (Figure 3). An analysis such as this can add value towards getting quick estimates of impacts as a function of gas compositions; the current literature primarily focuses on costs and scaling estimates based on NG and hydrocarbons.[36] Our past analysis included additional capital costs for reforming of PY gas by separately adding heat exchange network costs on top of literature estimates based on NG SMRs.[7] The hydrogen production rate is often the scaling variable for deriving costs of NG SMRs, but the granularity in this analysis to assess capital cost impacts on each individual operation may need to be adopted if NG substitution gains more commercial interest. Operating costs based on process modeling such as this can be reliable, if the configuration of interest is modeled correctly.

As also seen above, flow rates may be decreased by reducing S:C if CO_2 is a major component in PY gas, and the prereforming/reforming catalysts can utilize CO_2 instead of steam as the oxygen provider without adding to coking risk. The removal of CO_2 in PY gas can be another tool for reducing flow rates and system volume; as mentioned earlier, compatibility of CO_2 solvents with PY gas constituents need to be evaluated prior to adopting this approach. It should also be noted that there are cost, energy, and GHG penalties for CO_2 removal, and the benefits of CO_2 removal need to outweigh the penalties.

4. Conclusion

Renewable, but less energy-dense, oxygenated biogenic gases may be used to substitute NG and fossil hydrocarbons for the production of hydrogen. However, processing these gases in existing SMR-type designs may not always be optimal for hydrogen production, and processes need to be adjusted based on gas compositions; for example, a combination of CO_2 removal and WGS may be a good option for gases that have very high proportions of CO and CO_2. Alternate processes are also being considered for the conversion of biogenic gases to hydrogen.[6] Use of existing SMR setups with some adjustments may be enticing from capital and equipment reuse standpoints. While this can drive processes toward sustainability, larger equipment is necessary for the production of the same amount of hydrogen from less energy-dense gases; another option to boost sustainability using existing equipment is to reduce hydrogen production from the rated capacity (with NG feed) to help maximize GHG reduction; this may help achieve parity with the tiered emissions reductions targeted under the 45 V Clean Hydrogen Production Tax Credit introduced in the US.[43]

The key to efficient SMR processes while using oxygenated biogenic gases is to take advantage of the oxygen in both the feed and fuel trains. This is done more easily on the fuel side by reducing combustion air after accounting for the oxygen already present in the fuel gas. On the feed side dry reforming and development of suitable pre-reforming catalysts to reduce overall steam requirement can be one way to increase process efficiency. This analysis, with the assumed base case PY gas composition (Table 1) indicates that if sufficient PY gases are available at a location then, from a process standpoint, 100% replacement on fuel side and up to 25 mole % replacement on the feed side may be possible to

**ADVANCED
SCIENCE NEWS**

www.advancedsciencenews.com

**ADVANCED
SUSTAINABLE
SYSTEMS**

www.advsustainsys.com

achieve with relatively small modifications or within design tolerances of existing SMR systems. Greater than 25 mole % will likely require more extensive redesign or curtailment of the hydrogen production rate; note that threshold will change with gas compositions, e.g., low CO_2 in the gas and higher energy density will allow greater proportions of NG to be substituted. Another aspect, not considered in this analysis, is the potential for CO_2 sequestration to reduce emissions from the process. Any gas preprocessing, including CO_2 removal prior or after the process, will require additional equipment and energy use, and will have sustainability impacts that need to be included in any lifecycle and cost analysis. Note that this analysis focuses on impacts on process parameters; additional material and equipment changes may need to be considered in existing SMR systems based on gas compositions and properties (including potential corrosivity).

The design of future SMR plants may need to consider feed flexibility and necessary allowances if the supply of biogenic gases increases in the future; the development of versatile pre-reforming catalysts with low coking propensity, including dry-reforming capabilities can enable this aspect. Hydrogen is one potential bulk product from biogenic off-gases, and has the advantage of high future demand projections. Electricity production is another option, but will face competition from renewable solar and wind technologies that are already cost-competitive; on the other hand, hydrogen production via electrolysis is farther away from cost parity with SMR hydrogen. Production of syngas (also via steam reforming) from these biogenic gases for conversion of syngas to liquid fuels, including SAF, may be another use in line with future fuel demand projections. Effective utilization of biogenic gases to maximize sustainability impacts may also enable liquid fuel technologies for producing SAF from pyrolytic and other processes that are being implemented or under development; many of those efforts require further yield improvements to maximize SAF. Lower SAF and liquid fuel yields are typically complemented by more off-gas production, as is the case with pyrolysis processes, and renewable hydrogen production from those gases using known current technologies, such as SMRs, can be an effective use of the gases even as electrolytic processes for hydrogen progress toward commercialization.

Supporting Information

Supporting Information is available from the Wiley Online Library or from the author.

Conflict of Interest

The author declares no conflict of interest. Products or companies are named solely for descriptive clarity, and this neither constitutes nor implies endorsement or criticism by the author, NREL, or by the U.S. government.

Data Availability Statement

The data that support the findings of this study are available in the supplementary material of this article.

[1] D. Mohan, C. U. Pittman Jr., P. H. Steele, *Energy Fuels* **2006**, *20*, 848.

[2] United Nations, Department of Economic and Social Affairs, Sustainable Development, https://sdgs.un.org/goals (accessed: 2023).

[3] International Energy Agency (IEA), Hydrogen, Energy System Overview Tracking Report, https://www.iea.org/reports/hydrogen (accessed: May 2023).

[4] International Energy Agency (IEA), Hydrogen Supply, Subsector Overview, Tracking Report – September 2022, https://www.iea.org/reports/hydrogen-supply (accessed: May 2023).

[5] Hydrogen Strategy: Enabling a Low-Carbon Economy, Office of Fossil Energy, July 2020, https://www.energy.gov/sites/prod/files/2020/07/f76/USDOE_FE_Hydrogen_Strategy_July2020.pdf (accessed: May 2023).

[6] T. Marker, M. Linck, L. Felix, P. Ortiz-Toral, J. Wangerow, L. Kraus, C. McLeod, A. DelPaggio, E. Tan, J. Gephart, D. Gromov, I. Purtle, J. Starr, J. Hahn, P. Dorrington, J. Stevens, D. Shonnard, E. Maleche. Biomass to Gasoline and Diesel Using Integrated Hydropyrolysis and Hydroconversion, GTI Technical Report, December **2012**. Gas Technology Institute, Des Plaines, Illinois, https://www.osti.gov/servlets/purl/1059031 (accessed: May 2023).

[7] A. Dutta, A. Sahir, E. Tan, D. Humbird, L. Snowden-Swan, P. Meyer, J. Ross, D. Sexton, R. Yap, J. Lukas, *Process Design and Economics for the Conversion of Lignocellulosic Biomass to Hydrocarbon Fuels— Thermochemical Research Pathways with in Situ and Ex Situ Upgrading of Fast Pyrolysis Vapors, Report No: NREL/TP-5100-62455*, National Renewable Energy Laboratory, Golden, CO, **2015**, https://www.nrel.gov/docs/fy15osti/62455.pdf.

[8] T. Marker, Integration of IH2 with the Cool Reformer for the Conversion of Cellulosic Biomass to Drop-In Fuels. DOE-BETO Project Peer Review, March 25, 2021, https://www.energy.gov/sites/default/files/2021-04/beto-33-peer-review-2021-sdi-marker.pdf (accessed: May 2023).

[9] Sustainable Aviation Fuels: Review of Technical Pathways, Bioenergy Technologies Office, DOE/EE-2041, September 2020, https://www.energy.gov/sites/prod/files/2020/09/f78/beto-sust-aviation-fuel-sep-2020.pdf, (accessed: May 2023).

[10] A. Dutta, H. Cai, M. S. Talmadge, C. Mukarakate, K. Iisa, H. Wang, D. M. Santosa, L. Ou, D. S. Hartley, A. Nolan Wilson, J. A. Schaidle, M. B. Griffin, *Chem. Eng. J.* **2023**, *451*, 138485.

[11] A. Dutta, M. S. Talmadge, E. C. D. Tan, J. A. Schaidle, *Sustain Energy Fuels* **2023**, *7*, 4955.

[12] K. Chouhan, S. Sinha, S. Kumar, S. Kumar, *Int. J. Hydrogen Energy* **2021**, *46*, 26809.

[13] T. S. Phan, D. Pham Minh, F. Espitalier, A. Nzihou, D. Grouset, *Int. J. Hydrogen Energy* **2022**, *47*, 42027.

[14] M. Shamsi, S. Moghaddas, E. Naeiji, S. Farokhi, *Arab J Sci Eng* **2023**, *48*, 8971.

[15] F. Alrashed, U. Zahid, *Comput Chem Eng* **2021**, *154*, 107497.

[16] IEAGHG, Techno-Economic Evaluation of SMR Based Standalone (Merchant) Hydrogen Plant with CCS. Tech. Rev. 2017-02 286. Cheltenham: IEAGHG. 2017, https://ieaghg.org/exco_docs/2017-02.pdf.

[17] L. Herraiz, M. Lucquiaud, H. Chalmers, J. Gibbins, *Front. Energy Res.* **2020**, *8*, 180.

[18] X. D. Peng, *Ind. Eng. Chem. Res.* **2012**, *51*, 16385.

[19] X. Zhao, B. Joseph, J. Kuhn, S. Ozcan, *iScience* **2020**, *23*, 101082.

[20] E. F. Iliopoulou, S. Stefanidis, K. Kalogiannis, A. C. Psarras, A. Delimitis, K. S. Triantafyllidis, A. A. Lappas, *Green Chem.* **2014**, *16*, 662.

[21] K. Wang, D. C. Dayton, J. E. Peters, O. D. Mante, *Green Chem.* **2017**, *19*, 3243.

[22] M. B. Griffin, K. Iisa, H. Wang, A. Dutta, K. A. Orton, R. J. French, D. M. Santosa, N. Wilson, E. Christensen, C. Nash, K. M. Van Allsburg, F. G. Baddour, D. A. Ruddy, E. C. D. Tan, H. Cai, C. Mukarakate, J. A. Schaidle, *Energy Environ. Sci.* **2018**, *11*, 2904.

[23] K. J. Andersson, M. S. Rasmussen, P. E. H. Nielsen, *Fuel* **2017**, *203*, 1026.

[24] R. L. Bain, K. A. Magrini-Bair, J. E. Hensley, W. S. Jablonski, K. M. Smith, K. R. Gaston, M. M. Yung, *Ind. Eng. Chem. Res.* **2014**, *53*, 2204.

[25] A. Dutta, S. D. Phillips, *Thermochemical Ethanol via Direct Gasification and Mixed Alcohol Synthesis of Lignocellulosic Biomass*, NREL/TP-510-45913, National Renewable Energy Laboratory, Golden, CO **2009**.

[26] A. Dutta; M. Talmadge; J. Hensley, M. Worley, D. Dudgeon, D. Barton, P. Groenendijk; D. Ferrari; B. Stears, E. M. Searcy, C. T. Wright, J. R. Hess, *Process Design and Economics for Conversion of Lignocellulosic Biomass to Ethanol: Thermochemical Pathway by Indirect Gasification and Mixed Alcohol Synthesis*, Technical Report NREL/TP-5100-51400, National Renewable Energy Laboratory, Golden, CO, USA, **2011**.

[27] A. Dutta, R. L. Bain, M. J. Biddy, *Environ Prog Sustain Energy* **2010**, *29*, 163.

[28] J. Rostrup-Nielsen, I. Dybkjaer, L. J. Christiansen, in *Steam Reforming Opportunities and Limits of the Technology* (Eds.: H.I. de Lasa, G. Doğu, A. Ravella), NATO ASI Series 225, Springer, Dordrecht, **1992**.

[29] J. M. Smith, H. Van Ness, M. Abbott, M. Swihart, *Introduction to Chemical Engineering Thermodynamics*, 8th ed., McGraw Hill, New York **2017**.

[30] B. E. Poling, J. M. Prausnitz, J. P. O'Connell, *The Properties of Gases and Liquids*, 5th ed., McGraw Hill, New York **2000**.

[31] M. T. Azizan, A. Aqsha, M. Ameen, A. Syuhada, H. Klaus, S. Z. Abidin, F. Sher, *Biomass Convers Biorefin* **2020**, *13*, 8441.

[32] S. Bepari, D. Kuila, *Int. J. Hydrogen Energy* **2020**, *45*, 18090.

[33] J. R. Rostrup-Nielsen, T. Rostrup-Nielsen, *CATTECH* **2002**, *6*, 150.

[34] Aspen Plus Process Simulator Version 10, Aspen Technology, Inc., Bedford, MA. USA.

[35] P. Spath, A. Aden, T. Eggeman, M. Ringer, B. Wallace, J. Jechura, Biomass to Hydrogen Production Detailed Design and Economics Utilizing the Battelle Columbus Laboratory Indirectly Heated Gasifier, NREL/TP-510-37408, https://www.nrel.gov/docs/fy05osti/37408.pdf (accessed: May 2005).

[36] J. H. Gary, G. E. Handwerk, M. J. Kaiser, *Petroleum Refining: Technology and Economics*, 5th ed., CRC Press, Boca Raton, FL **2007**.

[37] R. Morissette, P. Savoie, J. Villeneuve, *Energies* **2011**, *4*, 1102.

[38] K. R. Ramakumar, Monitoring hydrogen plant performance - Part 1. Hydrocarbon Processing, October **2021**.

[39] European Industrial Gases Association (EIGA), Combustion Safety for Steam Reformer Operation, Doc 172/19.

[40] P. Basu, C. Kefa, L. Jestin, *Boilers and Burners*, Mechanical Engineering Series, Springer, New York, NY **2000**.

[41] K. R. Ramakumar, Monitoring hydrogen plant performance - Part 2. Hydrocarbon Processing, October **2021**.

[42] Greenhouse gases, Regulated Emissions, and Energy use in Technologies Model (GREET), **2022**, https://doi.org/10.11578/GREET-Net-2022/dc.20220908.2.

[43] Building a Clean Energy Economy: A Guidebook to the Inflation Reduction Act's Investments in Clean Energy and Climate Action, The White House, Washington, Version 2, **2023**, https://www.whitehouse.gov/wp-content/uploads/2022/12/Inflation-Reduction-Act-Guidebook.pdf.